

06,11

## Phase states of solid solution $(1 - x)\text{PbFe}_{0.5}\text{Nb}_{0.5}\text{O}_3 - x\text{PbTiO}_3$ . Description based on multimimum models

© M.P. Ivliev, S.I. Raevskaya, V.V. Titov, I.P. Raevski, M.A. Malitskaya

Southern Federal University, Research Institute of Physics,  
Rostov-on-Don, Russia

E-mail: ivlievmp@rambler.ru

Received December 2, 2022

Revised December 2, 2022

Accepted January 20, 2023

Based on the composition of two multimimum models, a statistical model has been developed on the basis of which the formation of tetragonal and monoclinic ferroelectric phases in a solid solution  $(1 - x)\text{PbFe}_{0.5}\text{Nb}_{0.5}\text{O}_3 - x\text{PbTiO}_3$  has been investigated and described. By selecting the parameters of the model, it was possible to reproduce the diagram  $T(x)$  of this solid solution. The peculiarity of the diagram is that when approaching the concentration of  $x \approx 0.1$ , the temperature of the phase transition between the tetragonal and monoclinic phases decrease sharply, turning to zero. It is shown that the disappearance of the monoclinic phase is due to the specifics of the statistical properties of the eight-minimum model describing the subsystem of octahedra with eight minima. The features of the thermodynamic properties of a solid solution in the vicinity of the morphotropic boundary between the tetragonal and monoclinic phases are also investigated.

**Keywords:** ferroelectrics, phase transitions, monoclinic phase, morphotropic boundary.

DOI: 10.21883/PSS.2023.04.55994.543

### 1. Introduction

Lead ferroniobate (PFN) is a ternary perovskite — a multiferroic with the general structural formula of  $AB'_{0.5}B''_{0.5}O_3$ , that has simultaneously ferroelectric (FE) and magnetic properties [1–3]. Also, in the FE-state PFN demonstrates elements of the relaxor behavior, which is partly related to the disordering in Fe and Nb cations distribution over B-sites of the perovskite [3–5].

Two macroscopic structural phase transitions (PhT) are observed in PFN. The first transition is between the paraelectric cubic phase (C-phase,  $\text{Pm}\bar{3}\text{m}$ ,  $\text{O}_h^1$ ) and the ferroelectric tetragonal phase (T-phase,  $\text{P4mm}$ ,  $\text{C}_{4v}^1$ ) at  $T \approx 376$  K and the second transition is between the ferroelectric tetragonal and monoclinic phases (M-phase,  $\text{Cm}$ ,  $\text{C}_s^3$ ) at  $T \approx 356$  K [1,2]. Phase transition to antiferromagnetically ordered phases take place at  $T \lesssim 140$  K [3]. The presence of a PhT between phases  $T$  and  $M$  (phase  $M$  is an intricately ordered monoclinic structure, which is close to a rhombohedral structure) suggests that in the solid solutions based on this material a morphotropic phase boundary can be formed, near which the compositions will have good piezoelectric and pyroelectric properties [6]. This circumstance allows considering the PFN as a promising basis for the design of new piezoactive and pyroactive materials that, in addition, have magnetoelectric properties. However, to achieve higher efficiency of the development process of materials that use some or other of special properties of the basic compound, the knowledge of formation mechanisms of these properties is needed. This will give the possibility of targeted impact on the properties to improve their quantitative and qualitative parameters.

As for the PFN, until recently, no any reasonable explanation has been presented for how and due to what such an unusual sequence of phase states (PS) is formed in this compound. A description of one of possible variant of the PS pattern formation in PFN has been presented only a short time ago in [5]. This study suggests a statistical model based on the composition of two interacting multimimum models: a six-minima model, i.e. a model with six crystallographically equivalent positions (CEP) for the Pb cation subsystem and an eight-minima model, i.e. a model with eight CEPs for the Nb cation subsystem.

The scenario of formation of phase states in the PFN based on the model suggested in [5] was assumed as follows. With a decrease in temperature, first a first-order PhT from the cubic phase to the tetragonal FE-phase should occur in the Pb cation subsystem with six CEPs. At the same time, due to the interaction between subsystems, also an order parameter (OP) characterizing the polarization along the  $C_4$  axis should occur in the Nb cation subsystem with eight CEPs. Therefore, with further decrease in temperature, the first-order phase transition to the rhombohedral (with „turned off“ interaction between subsystems) phase in the subsystem with eight CEPs is converted to the phase transition „in an external field“ of tetragonal symmetry; as a result, the rhombohedral phase becomes monoclinic. The selection of model parameters taking into account these conditions allowed simulating all typical features of thermodynamic behavior of the crystal, namely the emergence of ferroelectric and ferroelastic instabilities, formation of FE-phase states in a certain sequence, etc. [5].

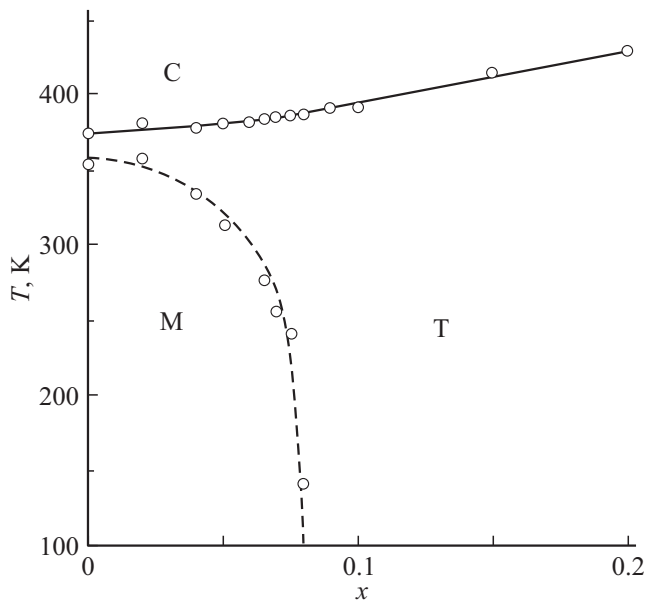


**Figure 1.** PS diagram of PFN- $x$ PT solid solution [7]. Phases C and T, as well as phases T and M (at  $x < 0.08$ ) have a border along the line of the first-order PhT, phases T and M (at  $x > 0.08$ ) have a border along the line of the second-order PhT.

As it is noted above, PFN can be considered as a promising basis for the creation of materials with high piezoactivity and pyroactivity. Accordingly, the next stage is the development of a modified model to study and describe thermodynamic properties of PFN-based solid solutions. The  $(1-x)\text{PbFe}_{0.5}\text{Nb}_{0.5}\text{O}_3 - x\text{PbTiO}_3$  (PFN- $x$ PhT) solid solution is considered as a model object. This choice is grounded by the circumstance that thermodynamic properties of this solid solution are investigated in a wide range of temperatures and concentrations, a diagram of phase states is built (Fig. 1) [7,8], which is a good basis for the development of a modified model and its testing for the ability to describe adequately the set of main experimentally established properties of the compound.

It can be seen in Fig. 1, that the diagram has a morphotropic phase boundary, and in the region of low  $x$  the monoclinic phase M has a structure, which is very close to a rhombohedral structure and at  $0.07 \lesssim x \leq 0.1$  phase M is very close to the tetragonal phase T [7,8]. The feature of this diagram is that as the concentration approaches  $x \approx 0.08$ , temperatures of phase transitions between the tetragonal phase and the monoclinic phase decrease abruptly and become equal to zero, and in the region of  $x > 0.08$  only the tetragonal phase exists and the monoclinic phase disappears. Similar PS patterns are observed in  $\text{PbZr}_x\text{Ti}_{1-x}\text{O}_3$ ,  $(1-x)\text{Pb}(\text{Mg}_{1/3}\text{Nb}_{2/3})\text{O}_3 - x\text{PbTiO}_3$ ,  $(1-x)\text{Pb}(\text{Zn}_{1/3}\text{Nb}_{2/3})\text{O}_3 - x\text{PbTiO}_3$  [9–12] ceramics with unique piezoelectric properties. Therefore, there is every expectation that PFN is a really promising basis for the creation of new piezoactive materials. Accordingly, the development of a modified model that is able to study

and describe how and due to what the phase states observed in PFN- $x$ PhT solid solutions are formed, is an important and vital task. Thus, this work is aimed at solving this task.

## 2. Description of the model

It has been shown in [5], that in a somewhat simplified variant cations in B-sites of a PFN crystal can be considered as averaged  $(\text{Fe/Nb})^{4+}$  cations. In the solid solution, these averaged cations are substituted by  $\text{Ti}^{4+}$  cations. PS diagram of PFN- $x$ PhT solid solutions looks like the diagram shown in Fig. 1 [7]. It can be seen in the diagram, that as the concentration of Ti grows, a relatively small growth of temperature of the C-T PhT and a sharp decrease in temperature of the T-M PhT occur. According to [5], this is an evidence of an increase in the contribution to thermodynamic characteristics of the crystal from the subsystem of ferroactive cations with six CEPs and a decrease in the contribution from the subsystem of ferroactive cations with eight CEPs. Thus, in a first approximation the substitution of  $(\text{Fe/Nb})^{4+}$  cation with  $\text{Ti}^{4+}$  cation can be interpreted as a replacement of an eight-CEP particle with a six-CEP particle.

In this case the nonequilibrium thermodynamic potential (TP) of the  $(1-x)\text{PFN}-x\text{PbTiO}_3$  system in the Gorsky-Bragg-Williams approximation [13,14] per one formula unit can be represented as follows [5]:

$$F_0(x) = F_6(x) + F_8(x) + H_{\text{int}}(x), \quad (1)$$

where  $F_6(x)$  is TP of the 6-minima model that describes orderings in the Pb cation subsystem and the Ti cation subsystem:

$$F_6(x) = \frac{(1+x)^2}{6} \left[ A_6 \left( \sum_{i=1}^3 \varepsilon_i^2 \right) + B_6 (6\gamma_1^2 + 2\gamma_2^2) \right] + T \sum_{k=1}^6 n_k \ln n_k, \quad (2)$$

$$n_{1,2} = \frac{1+x}{6} (1 + 2\gamma_1 \pm \varepsilon_1),$$

$$n_{3,4} = \frac{1+x}{6} (1 - \gamma_1 + \gamma_2 \pm \varepsilon_2),$$

$$n_{5,6} = \frac{1+x}{6} (1 - \gamma_1 - \gamma_2 \pm \varepsilon_3),$$

$F_8(x)$  is TP of the 8-minima model that describes orderings in the  $(\text{Fe/Nb})$  cation subsystem:

$$F_8(x) = \frac{(1-x)^2}{8} \left[ A_8 \left( \sum_{i=1}^3 \varphi_i^2 \right) + D_8 \left( \sum_{i=1}^3 e_i^2 \right) + G_8 \xi^2 \right] + T \sum_{i=1}^8 p_i \ln p_i, \quad (3)$$

$$\begin{aligned}
p_{1,2} &= \frac{1-x}{8} [1 + e_1 + e_2 + e_3 \pm (\xi + \varphi_1 + \varphi_2 + \varphi_3)], \\
p_{3,4} &= \frac{1-x}{8} [1 + e_1 - e_2 - e_3 \pm (\xi + \varphi_1 - \varphi_2 - \varphi_3)], \\
p_{5,6} &= \frac{1-x}{8} [1 - e_1 + e_2 - e_3 \pm (\xi - \varphi_1 + \varphi_2 - \varphi_3)], \\
p_{7,8} &= \frac{1-x}{8} [1 - e_1 - e_2 + e_3 \pm (\xi - \varphi_1 - \varphi_2 + \varphi_3)], \\
H_{\text{int}}(x) &= h(1-x)(1+x) \left( \sum_{j=1}^3 \varepsilon_j \varphi_j \right)
\end{aligned}$$

where  $x$  is concentration of titanium ions;  $A_6, A_8, B_6, B_8, G_8$  are functions of constants that characterize pair interactions, both direct and indirect, through the anion subsystem, between particles of the same type, and  $h$  is a function that characterizes pair interactions between particles of different types (in fact, all of them are phenomenological parameters of the theory);  $n, p$  are functions that characterize probabilities of CEP filling; „+“ sign is referred to odd numbers, and „-“ sign is referred to even numbers; numbering and arrangement of CEPs are shown in [5];  $\varepsilon, \gamma, \varphi, e, \xi$  variables serve as order parameters (OP),  $\varepsilon$  and  $\varphi$  characterize polarization in polyhedra with six CEPs and in octahedra with eight CEPs, respectively,  $\gamma \in E_g$  and is transformed as a tensor of uniaxial deformations,  $e \in T_{2g}$  and is transformed as a tensor of shear deformations,  $\xi \in A_{2u}$  and is transformed as a third-rank tensor of the  $xyz$  form.  $\varepsilon$  and  $\varphi$  order parameters, in fact, determine the polarization, and  $\gamma$  and  $e$  OPs determine uniaxial deformations and shear deformations of the crystal. Phases T and M are characterized by the following sets of OPs:  $\varepsilon_1, \varphi_1, \gamma_1$  and  $\varepsilon_1, \varepsilon_2 = \varepsilon_3, \varphi_1, \varphi_2 = \varphi_3, \gamma_1, e_2 = e_3, e_1, \xi$ , respectively. Values of these OPs are determined by the system of equations for states

$$\begin{aligned}
\frac{\partial F_0(x)}{\partial \varepsilon_i} = 0, \quad \frac{\partial F_0(x)}{\partial \gamma_i} = 0, \quad \frac{\partial F_0(x)}{\partial \xi} = 0, \\
\frac{\partial F_0(x)}{\partial e_i} = 0, \quad \frac{\partial F_0(x)}{\partial \varphi_i} = 0. \quad (4)
\end{aligned}$$

Equilibrium solutions are those that have an absolute minimum of  $F_0(x)$  correspondent to them at given values of  $x, A_6, A_8, B_6, D_8, G_8, h, T$ .

Using the relationships between the model parameters of  $A_8 = 3.6A_6, D_8 = 0.335A_8 = 1.206A_6, G_8 = 0, B_6 = 0.15A_6, h = 0.07A_6$  obtained in [5], a diagram of  $T(x)$  PSs can be built, that is described by the TP (1). In this case the line of the first-order PhT that separates phases C and T will have a shape close to that shown in Fig. 1. However, the boundary between phases T and M will be considerably different from the experimentally observed shape (Fig. 1). The analysis of stability conditions for phase T characterized by  $\varepsilon_1, \varphi_1, \gamma_1$  OPs in relation to the emergence of  $\varphi_2 = \varphi_3, e_2 = e_3$  OPs shows that with growth of  $x$  a gradual decrease takes place in the temperature of the PhT between phases T and M, however, both the phase M and the PhT remain in

the region of  $x \lesssim 1$ . However, it can be seen in Fig. 1, that temperature of the PhT between phases T and M decreases sharply with the growth of  $x$  and at  $x \approx 0.1$  it becomes equal to zero, and in the region of  $x > 0.1$  there is no phase M at all. Thus, a question arises about causes of such a dramatic decrease of temperature of this PhT and disappearance of the phase M. It can not be explained by a simple replacement of eight-CEP sites with six-CEP sites, as it has been shown. An assumption can be made that with the increase in  $x$  ( $x < 0.1$ ) the contribution from the subsystem with eight CEPs to the PS formation becomes lower, and at  $x > 0.1$  the above-mentioned subsystem stops the participation in this process. In this case, temperature of the PhT between phases C and T should surely decrease or at least its increment should become considerably less in the region of  $0 < x < 0.1$ , because the subsystem with eight CEPs promotes the increase in the temperature of this PhT through the  $\varphi$  order parameter. As the temperature of the PhT between phases C and T in Fig. 1 increases monotonously and almost linearly with increase in  $x$ , it can be said that the subsystem with eight CEPs, even at  $x > 0.1$ , continues to contribute to the formation of PE-phase state corresponding to the phase T, however, the PhT to the phase of pseudorhombohedral symmetry disappears. This suggests that at  $x > 0.1$  a tetragonal FE-phase emerges in the subsystem with eight CEPs instead of the rhombohedral phase. Indeed, the PS diagram of the eight-minima model described by  $F_8(x=0)$  TP, which general view is given in [15], in the region of  $A_8 < D_8 \leq 0$  has the only ordered FE-phase with the R3m rhombohedral symmetry, and in the region of  $A_8 < 0, D_8 > 0$  in addition to the rhombohedral phase, a tetragonal FE-phase with the P4mm symmetry appears. The emergence of the tetragonal FE-phase is related to the fact that in the region of  $A_8 < 0, D_8 > 0$  the FE-instability is remained, the  $\varphi$  OP remains critical but the contribution from the  $e$  OP should decrease, therefore the type of ordering changes: thus, in the rhombohedral phase R3m  $\varphi_1 = \varphi_2 = \varphi_3, e_1 = e_2 = e_3, \xi$  at  $D_8 \leq 0$ , and in the tetragonal phase P4mm —  $\varphi_1, \varphi_2 = \varphi_3 = e_1 = e_2 = e_3 = \xi = 0$  at  $D_8 > 0$ .

So, the disappearance of the monoclinic phase at  $x > 0.1$  may be due to the fact that the  $D_8$  parameter becomes dependent on  $x$  and with increase in  $x$  it changes its sign and becomes positive. As a result, in the subsystem with eight CEPs a FE-tetragonal phase is formed instead of the FE-rhombohedral phase. By fitting, a dependence of  $D_8$  on  $x$  was established that allows simulating the shape of boundary between phases T and M close to that observed in the experiment. By assuming that

$$\begin{aligned}
A_8 = 3.6A_6, \quad D_8(x) = (1 + 6x - 458.5x^2) \cdot 0.335 \cdot 3.6A_6, \\
G_8 = 0, \quad B_6 = 0.15A_6, \quad h = 0.07A_6,
\end{aligned}$$

the shape shown in Fig. 2 is obtained for the  $T(x)$  PS diagram described by TP (1).

It can be seen in the diagram, that with increase in  $x$  the temperature of the first-order PhT between phases C and T

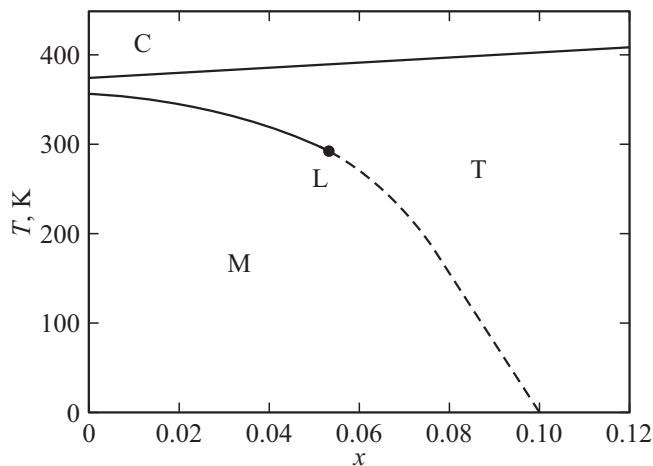


**Figure 2.** PS diagram described by TP (1). Boundary between phases C and T — the line of the first-order PhT. L point is a tricritical point ( $x \approx 0.05$ ), where the line of the first-order PhT between phases T and M (solid line) joins the line of the second-order PhT (dashed line).

grows and the temperature of the PhT between phases T and M decreases. In the region of  $x < 0.05$  phases T and M have a boundary along the line of the first-order PhT, and in the region of  $0.05 < x < 0.1$  they have a boundary along the line of the second-order PhT. In the tricritical point L ( $x \approx 0.05$ ) the first-order PhT is transformed to the second-order PhT. It means, that in the region of  $x > 0.05$  at the T–M phase transition in the plane normal to the  $C_4$  polar axis strong anomalies of permittivity will be observed.

With increase in  $x$ , increases the temperature interval between phases C and M, where phase T exists. Thus, at  $x = 0.02$  the temperature of the C–T phase transition ( $T_{CT}$ ) is 381 K, and the temperature of the T–M phase transition is  $T_{TM} = 348$  K. At the T–M phase transition OPs change as follows: in phase T —  $\varepsilon_1 = 2.42$ ,  $\varphi_1 = 0.6$ ,  $\gamma_1 = 0.73$  ( $\varepsilon_{1\max} = 3$ ,  $\varphi_{1\max} = 1$ ,  $\gamma_{1\max} = 1$ ); in phase M —  $\varepsilon_1 = 2.43$ ,  $\varepsilon_2 = 0.02$ ,  $\varphi_1 = 0.63$ ,  $\varphi_2 = 0.27$ ,  $\gamma_1 = 0.73$ ,  $e_1 = 0.1$ ,  $e_2 = 0.2$ ,  $\xi = 0.08$ . At  $x = 0.04$  —  $T_{CT} = 386$  K,  $T_{TM} = 322$  K. At the T–M phase transition: in phase T —  $\varepsilon_1 = 2.67$ ,  $\varphi_1 = 0.68$ ,  $\gamma_1 = 0.84$ ; in phase M —  $\varepsilon_1 = 2.67$ ,  $\varepsilon_2 = 0.006$ ,  $\varphi_1 = 0.69$ ,  $\varphi_2 = 0.14$ ,  $\gamma_1 = 0.82$ ,  $e_1 = 0.02$ ,  $e_2 = 0.1$ ,  $\xi = 0.02$ . The phase transition from phase T to phase M is due to the condensation of the critical OP:  $\varphi_2$ . At  $x = 0.02$  and  $x = 0.04$  this OP appears in a „hopwise“ manner —  $\Delta\varphi_2 = 0.27$  and  $\Delta\varphi_2 = 0.14$ , respectively. In addition, with increase in  $x$  the  $\varphi_1 - \varphi_2$  difference grows, therefore, with the transition the degree of phase M closeness to the rhombohedral phase decreases. Also, with increase in  $x$  the „radicality“ of the T–M phase transition decreases, and at  $x \geq 0.05$  the phase transition becomes continuous.

It is necessary to note that a similar pattern can be observed in the experiment as well. Thus, in [7,8] it was noted, that in the region of  $x < 0.08$  the transition

between phases M and T is accompanied by a temperature hysteresis, which magnitude decreases with growth of  $x$ . In addition, it can be seen on the graph of the  $V^{1/3}(x)$  dependence obtained at  $T \approx 300$  K, that in the region of  $x \approx 0.06$  an anomaly exists that corresponds to the T–M first-order phase transition [7]. The hysteresis disappears at  $0.08 < x \leq 0.1$  and at  $x \lesssim 0.08$  the PhT between phases T and M becomes continuous, and at the T–M interphase boundary there is a tricritical point at  $x \approx 0.08$ , where the line of the first-order PhT is converted to the line of the second-order PhT.

### 3. Results and discussion

Key factors determining the formation of PS pattern in the PFN– $x$ PhT solid solution can include the following. With increase in  $x$  a substitution of  $(\text{Fe/Nb})^{4+}$  eight-CEP cation with  $\text{Ti}^{4+}$  six-CEP cation takes place. At the same time, the  $D_8$  constant that characterize interaction of  $e$  order parameters becomes dependent on  $x$ , and as  $x$  increases it changes sign and becomes positive. As a result, in the subsystem of cations with eight CEPs a FE-tetragonal phase emerges instead of the FE-monoclinic phase (the rhombohedral phase in the case of turned off interaction between subsystems). By fitting, it was established that the coefficient characterizing the dependence of  $D_8$  on  $x$  can be represented in the following form:  $1 + 6x - 458.5x^2$ . With small  $x$  this coefficient increases very insignificantly ( $D_8(x) < 0$ ), then, with increase in  $x$ , it decreases and at  $x \approx 0.054$  it becomes zero ( $D_8(x) = 0$ ), and at  $x \approx 0.1$  it becomes equal to  $-2.985$  ( $D_8(x) > 0$ ).

The  $\varphi$  order parameters characterize dipole component in the cation distribution over eight CEPs, i.e. the dipole moment of the cation density distribution. Similarly, the  $e$  OPs characterize quadrupole moment of the distribution, which is similar to shear deformations in terms of symmetry. It follows from the analysis of eight-minima model properties, that at  $D_8(x) < 0$  the presence of  $e$  order parameters decreases energy of the system, therefore at  $x = 0$  the critical OP, i.e.  $\varphi$ , is condensed in such a way that its emergence is accompanied by appearance of secondary (accompanying) OPs:  $e$ . In this case both dipole moments and quadrupole moments described by  $\varphi$  and  $e$  order parameters become ordered. In this way the FE-rhombohedral phase  $\varphi_1 = \varphi_2 = \varphi_3$ ,  $e_1 = e_2 = e_3$ ,  $\xi$  is formed. At  $D_8(x) > 0$  the presence of  $e$  OP increases energy of the system, therefore the critical OP, i.e.  $\varphi$ , is condensed in such a way that excludes  $e$  secondary OPs, i.e. to the tetragonal phase  $\varphi_1, \varphi_2 = \varphi_3 = e_1 = e_2 = e_3 = \xi = 0$ .

Thus, with the increase in  $x$  from 0 up to 0.1 on the background of FE-ordering ( $|\varphi| \neq 0$ ) the nature of the interaction between quadrupole moments changes radically, from the trend to ordering ( $e \neq 0$ ) to the trend to disordering ( $e = 0$ ). The question about causes of this change requires an individual investigation. Therefore, without

going deep in details, a number of factors should be noted that may be responsible for this process.

The substitution of  $(\text{Fe/Nb})^{4+}$  cations with  $\text{Ti}^{4+}$  cations leads to an increase in the mean distance between cations with eight CEPs, which is accompanied by a decrease in the interaction between  $e$  OPs. Also, it is necessary to note, that octahedra with six CEPs are weakly susceptible to impacts induced by  $e$  OPs because positions of the [111] type correspond to the maximum of potential energy of the  $\text{Ti}^{4+}$  cation inside the oxygen octahedron. Therefore, the  $\text{TiO}_6$  octahedra make significantly weaker the interactions between  $e$  OPs. However, it is obviously insufficient for such a sharp change in the nature of their interaction.

Another important factor is the specifics of the interaction between the substituting  $\text{Ti}^{4+}$  cation and neighboring  $(\text{Fe/Nb})^{4+}$  cations. In crystals with perovskite structure, two neighbor octahedra have one common vertex. Therefore, the interaction of the  $\text{TiO}_6$  octahedron with six neighbor  $(\text{Fe/Nb})\text{O}_6$  octahedra is an interaction of antiferrodistortive type. With this type of interaction between neighbor cations repulsion can arise between CEPs of the same type (i.e. CEPs with the same arrangement [5]) and attraction can arise between CEPs of different types. With increase in  $x$ , units formed by  $\text{Ti}^{4+}$  cations and their closest neighbors, the  $(\text{Fe/Nb})\text{O}_6$  octahedra, become closer to each other. As the units become closer to each other, the degree of disordering in the subsystem of octahedra with eight CEPs increases. The disordering mainly covers CEPs 1, 3, 6, 8 (3) [5], so that the  $e$  OP decreases and the  $\varphi_1$  OP remains nearly unchanged because its value is kept by the interaction with the  $\varepsilon_1$  OP that characterizes the FE-ordering in subsystems of  $\text{Pb}^{2+}$  and  $\text{Ti}^{4+}$  cations. At  $x \approx 0.1$ , the mean distance between  $\text{Ti}^{4+}$  cations becomes equal to about  $2a$  (lattice constant  $\approx 4 \text{ \AA}$ ), therefore the abovementioned units start to be overlapped with each other strengthening the repulsion and suppressing the attraction between CEPs of the same type. Accordingly, in the region of  $x \lesssim 0.1$  probabilities of filling of CEPs 1, 3, 6, 8 become equal to each other —  $p_1 = p_3 = p_6 = p_8 = [(1-x)/8](1 + \varphi_1)$ , and the  $e$  OP becomes equal to zero.

Thus, if the first two of the abovementioned factors promote weakening of the interaction between  $e$  OPs, the last factor determines the significant change in the nature of the interaction between  $e$  order parameters, which results in their zeroing. This factor depends on the arrangement and the interaction of neighboring units, which determines the presence of the quadrupole term in the coefficient of the  $D_8$  constant.

Also, it is necessary to note some features of thermodynamic properties of the  $\text{PFN}-x\text{PhT}$  solid solution near the morphotropic interphase T–M–boundary. The specifics of the T–M–transition is that the condensation of the  $\varphi_2 = \varphi_3$  OP generates a set of OPs:  $\varepsilon_2 = \varepsilon_3 \approx \varphi_2 = \varphi_3$ ,  $e_2 = e_3 \approx \varphi_1\varphi_3 = \varphi_1\varphi_2$ ,  $e_1 \approx \varphi_2\varphi_3$ ,  $\xi \approx \varphi_1\varphi_2\varphi_3$ . In turn, the appearance of  $e$  order parameters is accompanied by the appearance of homogeneous shear deformations:  $u_{12} = u_{13} \approx e_2$ ,  $u_{23} \approx e_1$  [5]. It means, that in the case

of T–M–transition, due to  $\varphi_1 \neq 0$ , the  $e_2 = e_3$  OPs and the  $u_{12} = u_{13}$  shear deformations are pseudoeigen parameters of the PhT, i.e. they are parameters that are to the critical OP. Therefore, in the case of T–M–transition in the region of  $x > 0.05$ , in addition to the abovementioned anomaly of the permittivity, also an anomaly in the temperature dependence of the elastic modulus  $c_{44}$  will be observed, however, it will be significantly less manifested. In addition, near the morphotropic interphase T–M–boundary from the side of phase T described by  $\varepsilon_1$ ,  $\varphi_1$ ,  $\gamma_1$  OPs, the PhT to phase M can be initiated by applying external electric field in the direction of  $x = y$  (i.e. along the  $\varphi_2 = \varphi_3$ ) in the plane normal to the  $C_4$  polar axis (the  $z$  axis). The magnitude of the critical field  $E_c$ , that initiates the PhT, will be dependent on  $x$  and on the degree of closeness to the boundary. With  $0 \leq x \lesssim 0.05$  the  $E_c$  at the boundary is not zero, with increase in  $x$  it decreases and becomes zero at  $x \approx 0.05$ . In the region of  $0.05 < x \leq 0.1$  the  $E_c$  at the boundary is zero. Also, in the same way the PhT from phase T to phase M can be initiated using shear stresses connected with the deformations of  $u_{12} = u_{13}$  ( $u_{zx} = u_{zy}$ ), because  $u_{12} = u_{13}$  are pseudoeigen parameters of the PhT.

## 4. Conclusion

Based on the developed statistic-thermodynamic model taking into account the specifics of formation of  $\text{PFN}-x\text{PhT}$  solid solutions, main typical features and their thermodynamic behavior are successively investigated and described. It is found that the pattern of phase states in the solid solution is formed as follows. The substitution of  $(\text{Fe/Nb})^{4+}$  cations with  $\text{Ti}^{4+}$  cations leads to an increase in the contribution to the thermodynamic characteristics of the crystal from the subsystem with six CEPs and a decrease of the contribution from the subsystem with eight CEPs. As a result, the temperature of the PhT between the cubic phase and the tetragonal phase increases, and the temperature of the PhT between the tetragonal phase and the monoclinic phase decreases. As the  $x$  increases, the constant characterizing the interaction of  $e$  OPs changes its sign and becomes positive. Therefore, in the subsystem of cations with eight CEPs (with „turned off“ interaction with the six-CEP subsystem) the partially disordered tetragonal phase becomes the stable FE-phase instead of the rhombohedral phase. „Turning on“ the interaction between subsystems stabilizes the tetragonal phase, which remains stable at all  $x \leq 1$ , and the monoclinic phase disappears at  $x \lesssim 0.1$  (Fig. 2). One of important factors determining the significant change in the nature of the interaction between  $e$  OPs is the mutual influence of units formed by the substituting ferroactive  $\text{Ti}^{4+}$  cation and neighbor  $(\text{Fe/Nb})^{4+}$  cations. As the  $x$  increases, the mutual influence of units leads to disordering in the subsystem of octahedra with eight CEPs, such that the  $e$  OP decreases and becomes zero at  $x \approx 0.1$ , and the  $\varphi_1$  OP remains.

Taking into account results of [5] and results of this study, a conclusion can be made that the approach based on the multim minima model, despite significant simplifications, allows giving quite illustrative representation of the PS formation in PFN and in PFN- $x$ PhT, as well as identifying factors responsible for these processes. In particular, using the model approach, previously [5] it has been shown how and due to what the intricately ordered FE-monoclinic phase is formed. In this study, it was demonstrated by the example of the PFN- $x$ PhT solid solution how the basic model of [5] can be modified to investigate and describe thermodynamic properties of solid solutions. At the same time, it was demonstrated that the abrupt decrease of the temperature of the PhT between the tetragonal FE-phase and the monoclinic FE-phase down to zero and the disappearance of the monoclinic phase in the region of  $x > 0.1$  are due to the specifics of statistical properties of the eight-minima model [15], that describes the subsystem of octahedra with eight CEPs.

In addition, it is necessary to note that all results of the model analysis of features of thermodynamic properties of the solid solution in the surrounding of the morphotropic T-M boundary, with appropriate correction of  $x$  (i.e.  $x_L \approx 0.08$  must be used instead of  $x_L \approx 0.05$ ) are completely compliant with properties of the real solid solution (Fig. 1).

## Funding

The study was supported by the Ministry of Science and Higher Education of the Russian Federation [State assignment in the field of scientific activity, Southern Federal University, 2023, scientific project No. FENW-2023-0015].

## Conflict of interest

The authors declare that they have no conflict of interest.

## References

- [1] V. Bonny, M. Bonin, P. Sciau, K.J. Schenk, G. Chapuis. *Solid State Commun.* **102**, 5, 347 (1997).
- [2] N. Lampis, P. Sciau, A. Geddo-Lehmann. *J. Phys.: Condens. Matter* **11**, 17, 3489 (1999).
- [3] A. Falqui, N. Lampis, A. Geddo-Lehmann, G. Pinna. *J. Phys. Chem. B* **109**, 48, 22967 (2005).
- [4] S.A. Ivanov, R. Tellgren, H. Rundlof, N.W. Thomas, S. Ananta. *J. Phys.: Condens. Matter* **12**, 11, 2393 (2000).
- [5] M.P. Ivliev, S.I. Raevskaya, V.V. Titov, I.P. Raevski. *Phys. Solid State* **64**, 12 2034 (2022).
- [6] M. Ahart, M. Somayazulu, R.E. Cohen, P. Ganesh, P. Dera, H.-K. Mao, R.J. Hemley, Y. Ren, P. Liermann, Z. Wu. *Nature* **451**, 7178, 545 (2008).
- [7] I.P. Raevski, S.P. Kubrin, S.I. Raevskaya, S.A. Prosandeev, M.A. Malitskaya, V.V. Titov, D.A. Sarychev, A.V. Blazhevich, I. Zakharchenko. *IEEE Trans. Ultrason. Ferroelect. Freq. Control* **59**, 9, 1872 (2012).
- [8] S.P. Singh, S.M. Yusuf, S. Yoon, S. Baik, N. Shin, D. Pandey. *Acta Mater.* **58**, 16, 5381 (2010).
- [9] B. Noheda, J.A. Gonzalo, L.E. Cross, S.-E. Park, D.E. Cox, G. Shirane. *Appl. Phys. Lett.* **74**, 14, 2059 (1999).
- [10] B. Noheda, J.A. Gonzalo, L.E. Cross, R. Guo, S.-E. Park, D.E. Cox, G. Shirane. *Phys. Rev. B* **61**, 13, 8687 (2000).
- [11] B. Noheda, D.E. Cox, G. Shirane, R. Guo, B. Jones, L.E. Cross. *Phys. Rev. B* **63**, 1, 014103 (2001).
- [12] Z.-G. Ye, B. Noheda, M. Dong, D. Cox, G. Shirane. *Phys. Rev. B* **64**, 18, 184114 (2001).
- [13] W. Gorsky. *Z. Physik* **50**, 64 (1928).
- [14] W.L. Bragg, E.J. Williams. *Proc. R. Soc. A* **145**, 855, 699 (1934).
- [15] M.P. Ivliev, S.I. Raevskaya, I.P. Raevski, V.A. Shuvaeva, I.V. Pirog. *Phys. Solid State* **49**, 4, 769 (2007).

*Translated by Y.Alekseev*